Ab Initio Study of Cis−Trans Photoisomerization in Stilbene and Ethylene

Jason Quenneville and Todd J. Martínez*

Department of Chemistry and The Beckman Institute, University of Illinois, Urbana, Illinois 61801

Received: May 15, 2002; In Final Form: November 13, 2002

The photochemistry of stilbene is investigated using ab initio quantum chemistry with complete active space self-consistent field (CASSCF) and multireference perturbation theory (CASPT2) methods. We characterize photoisomerization pathways from both the cis and trans isomers, including a minimal energy conical intersection. Similarities to photoisomerization in ethylene are found and emphasized. In contrast to traditional one-dimensional models of stilbene photoisomerization, torsion and pyramidalization are required to reach the minimal energy conical intersection which is expected to dominate in quenching to the ground electronic state. This intersection is characterized as an interaction between charge transfer and covalent states. The present results suggest that the qualitative features of the photoisomerization dynamics elucidated for ethylene can also be expected to apply to stilbene, and call for reconsideration and refinement of the photoisomerization mechanism in stilbene.

Introduction

As one of the simplest means of converting light into mechanical motion on the angstrom scale, photoinduced cis-trans isomerization about double bonds has long been a subject of intense research. The conventional picture of this process has been a two-state, one-dimensional model, stressing torsional motion as the primary nuclear coordinate. At least in the case of ethylene, the smallest unsaturated hydrocarbon, this model is somewhat unsatisfactory. Ab initio electronic structure theory methods predict that the minimum electronic energy gap for ethylene in D_{2d} symmetry is approximately 60 kcal/mol, implying a long excited-state lifetime. Yet, no appreciable fluorescence is emitted by ethylene upon $\pi \rightarrow \pi^*$ excitation, and subpicosecond lifetimes have been measured by ultrafast spectroscopic techniques for longer polyenes such as hexatriene[1−8] and *cis*-stilbene.[9−11] Indeed, recent pump−probe experiments have measured lifetimes shorter than 100 fs for ethylene.[12,13] We have previously shown that one must be careful in the interpretation of these experiments,[14] but the fact remains that there is ample evidence for subpicosecond lifetimes which are most easily explained by regions of small or vanishing electronic energy gap.

Even before the accumulation of ultrafast data for unsaturated hydrocarbons, Michl speculated that a second coordinate might be involved, leading to a conical intersection that could promote radiationless decay.[15] The HCH angle was suggested as a possible candidate for this second coordinate. While it has turned out that this is not the correct coordinate, it has become clear that the minimal predictive model is two-dimensional, as discussed below.

We have recently reported on the first ab initio quantum molecular dynamics simulations of photoinduced cis−trans isomerization in ethylene.[14,16,17] Our results led to the proposal of an alternative model for photoinduced isomerization in ethylene, involving three electronic states (N, V, and Z in Mulliken notation), two nuclear coordinates (twisting and pyramidalization), and dominated by a conical intersection at a twisted, mono-pyramidalized geometry. A question immediately arises as to the generality of the model. Because ethylene is so short, one might wonder whether the photoinduced isomerization process is somehow different in ethylene and longer unsaturated hydrocarbons. Recent calculations by Roos and co-workers[18] imply that the same features we have stressed in ethylene are important also in the photodynamics of styrene, i.e., phenylethylene. In particular, they found that pyramidalization of the CH_2 group after twisting about the ethylenic double bond led to a conical intersection, analogous to our results for ethylene. However, the situation remains unclear because they did not search for minimal energy conical intersections and no dynamics was performed. Furthermore, pyramidalization was observed on the methylene side of the molecule, leaving open the possibility that the picture developed for ethylene breaks down when both of the ethylenic carbons are substituted.

Largely because it is brightly colored and absorbs light in an experimentally convenient region, the molecule which has served as an experimental paradigm for photoinduced cis−trans isomerization is stilbene−1,2-diphenylethylene. The theoretical framework which has dominated discussion of stilbene photochemistry centers on a one-dimensional reaction coordinate which is primarily torsional.[19−22] Nevertheless, some evidence of a more complicated reaction coordinate has been presented for the trans[23,24] isomer. Even more evidence of the inadequacy of a one-dimensional model is available for the cis[25−33] isomer. This is partially expected because steric repulsion forces the ground-state geometry of the cis isomer to be nonplanar, and both photoisomerization and photocyclization pathways can be accessed from the cis isomer.[30,34−37] Some theoretical studies of photodynamics in the cis isomer have allowed for degrees of freedom beyond simple torsion,[38−43] but these have emphasized phenyl rotation and the pyramidalization coordinate which we found to be important in ethylene has gone mostly unnoticed. In this paper, we investigate the ground- and excited-state potential energy surfaces (PESs) of stilbene in order to assess the generality of the model we have proposed for ethylene. We present multidimensional plots of the PESs that can be compared

* Corresponding author. Phone: 217-333-1449. E-mail: tjm@spawn.scs.uiuc.edu.

10.1021/jp021210w CCC: $25.00
Published on Web 01/15/2003

SCHEME 1

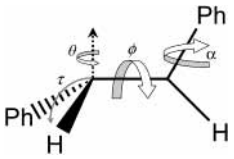

SCHEME 2

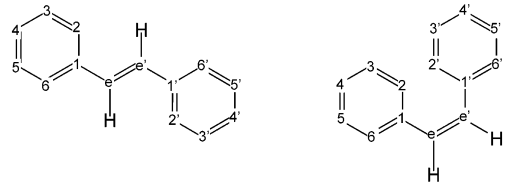

directly to our previous work on ethylene. The similarities are striking and provide strong support for the hypothesis that ethylene does represent a faithful prototype of photoisomerization mechanisms, especially when taken in conjunction with Roos' results for styrene.

Here we focus on aspects of the ground and excited electronic surfaces important to electronic state population quenching for *cis*- and *trans*-stilbene along the isomerization reaction coordinates. We do not specifically address the barriers to ethylenic torsion which play a role in *trans*-stilbene photochemistry, nor the DHP reaction coordinate, which is a minor product channel for the cis isomer.[34] The torsional barrier from the trans isomer is very important to the many studies which have used photoinduced isomerization of *trans*-stilbene in gas phase, cluster, and condensed phase environments as a benchmark system for studying statistical rate theories and intramolecular vibrational energy redistribution.[44−59] These details are left for future publication.

Results

We have used the MOLPRO quantum chemistry package[60] to carry out all calculations reported here. No symmetry restrictions were imposed on the electronic wave functions or molecular geometries and the 6-31G basis set was used.[61] Additionally, several of the important geometries have been verified using the polarized 6-31G** basis set.[62] A few important angles which will be used throughout this paper are depicted in Scheme 1.

The twist angle ϕ is the primary coordinate expected to be involved in the photoisomerization mechanism. The phenyl rotation angle α is especially important for the cis isomer, as this is a primary means of relieving the steric repulsion between the phenyl rings. The tilt and pyramidalization, θ and τ, as depicted are well-defined only for idealized geometries. Given an arbitrary geometry with no symmetry, we determine these angles by a least-squares fit to idealized geometries where a planar molecule with the same bond lengths is first twisted, then pyramidalized, and finally tilted. Unfortunately, there is no universally agreed-upon definition of the pyramidalization angle,[63] so we note that our definition gives $\tau = 0°$ for the planar carbon atom in methyl cation and $\tau = 55°$ for the purely tetrahedral carbon atom in methane. State-averaged[64] CASSCF wave functions[65] were employed in order to avoid a variational bias to any particular electronic state, abbreviated as SA-*N*-CAS(*n*/*m*), where *N* refers to the number of states included in the average while *n* and *m* are the number of active electrons and orbitals, respectively. As shown in Scheme 2, we label the ethylenic carbons as C_e and $C_{e'}$, the ethylenic hydrogens as H_e and $H_{e'}$, and the atoms of the phenyl rings as C_{1-6}, H_{2-6}, $C_{1'-6'}$, and $H_{2'-6'}$.

All geometry optimizations were performed at the SA-2-CAS-(2/2) level, and in some cases were repeated with SA-2-CAS-(14/12). The highest occupied and the lowest unoccupied molecular orbitals (HOMO and LUMO) are π- and π^*-type. Therefore the active space consisted of the π^2, $\pi\pi^*$, and π^{*2} configurations. Wave functions were further improved by extending the active space to include contributions from phenyl-ring π and π^* molecular orbitals in the larger CAS(14/12) calculations.

On the ground state, we found minima corresponding to the trans and cis isomers pictured in Figures 1 and 2, respectively. While both minima are of approximate C_{2v} symmetry, neither structure is planar. Steric effects force the cis isomer to be slightly twisted ($C_1-C_e-C_{e'}-C_{1'}$ dihedral angle of 6°) with its phenyl groups rotated 40° out-of-plane ($C_2-C_1-C_e-C_{e'}$ dihedral), consistent with the gas-phase experimental[66] values of 5° and 43°. The $S_1 \leftarrow S_0$ excitation energies computed using SA-2-CAS(2/2) for the cis and trans isomers are 6.07 eV and 5.74 eV, respectively. These values can be compared to the experimental absorption maxima for the $\pi \rightarrow \pi^*$ transition in hexane solution of 4.59 and 4.13 eV.[67] Part of the discrepancy in the vertical excitation energy is certainly due to the lack of dynamical electron correlation in the ab initio method used. We have carried out several calculations which include dynamic correlation in order to further characterize this discrepancy, and it appears that part of the problem is closely associated with the question of planarity in the S_0 equilibrium geometry, especially for the trans isomer. Indeed, Roos and co-workers[68] have achieved good agreement with experimental vertical transition energies for the trans isomer by assuming a planar S_0 geometry and using multireference perturbation theory (CASPT2). However, the planarity issue has been a source of some controversy,[37,59,69−82] and here we only comment that the vertical excitation energy is sensitive to the degree of phenyl rotation and the global minimum we located for the trans isomer has the phenyl rings rotated out of plane by 18° as shown in Figure 1. A future publication will address the effects of phenyl rotation on vertical excitation energies in detail. For now, we point out that the wave functions used are expected to provide an accurate depiction of the global character of the PESs, even if quantitative details such as the Stokes' shift are too large.[83,84] The *trans*-stilbene isomer is more stable than the cis isomer ($E_{\text{cis}\rightarrow\text{trans}} = 4.83$ kcal/mol), with $\Delta H^{0\,\text{K}}_{cis\rightarrow trans} = 4.78$ kcal/mol. This compares well with experimental measurements which found $\Delta H^{298\,\text{K}}_{cis\rightarrow trans} = 4.59$ kcal/mol in benzene solution.[85]

Geometrical parameters of the global energy minimum on S_1 are given in Figure 3. The molecule is twisted ($\phi = 107°$) and noticeably pyramidalized ($\tau = 32°$). Although we find the global minimum to be pyramidalized, it is important to note that the S_1 PES is quite flat with respect to this coordinate. Constraining the geometry so as to completely remove pyramidalization and minimizing on S_1 gives a purely twisted geometry and raises the excited-state energy by less than 3 kcal/mol. The energy difference of the S_0 and S_1 states at the global minimum is predicted to be 1.92 eV at the SA-2-CAS(2/2) level. This last result contrasts with ethylene, where, in similar ab initio studies,[83] no true global minimum was found on the first excited state. Instead, the points of lowest energy on the S_1 surface of ethylene correspond to conical intersections, accounting for the femtosecond lifetime of the excited molecule.[14,16,17]

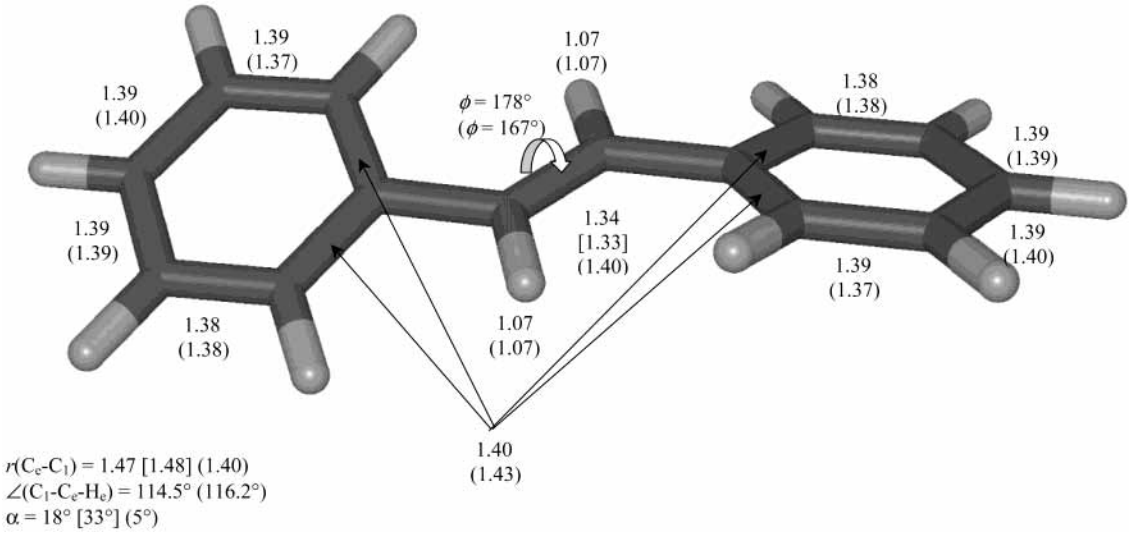

Figure 1. The ground-state equilibrium geometry in the trans conformation, optimized at the SA-2-CAS(2/2) level. Geometrical parameters in parentheses are for the trans-like minimum on the lowest $\pi\rightarrow\pi^*$ excited electronic state, which is S_1 at this level of theory. Experimental values from gas-phase electron diffraction[72] are given in square brackets. Note the nonplanarity of the S_0 minimum due to propeller-like twisting of the phenyl groups. At the S_1 trans minimum the molecule is slightly twisted about the ethylenic bond, and $C_1-C_e-C_{e'}-C_{1'}$ bond length alternation is lost.

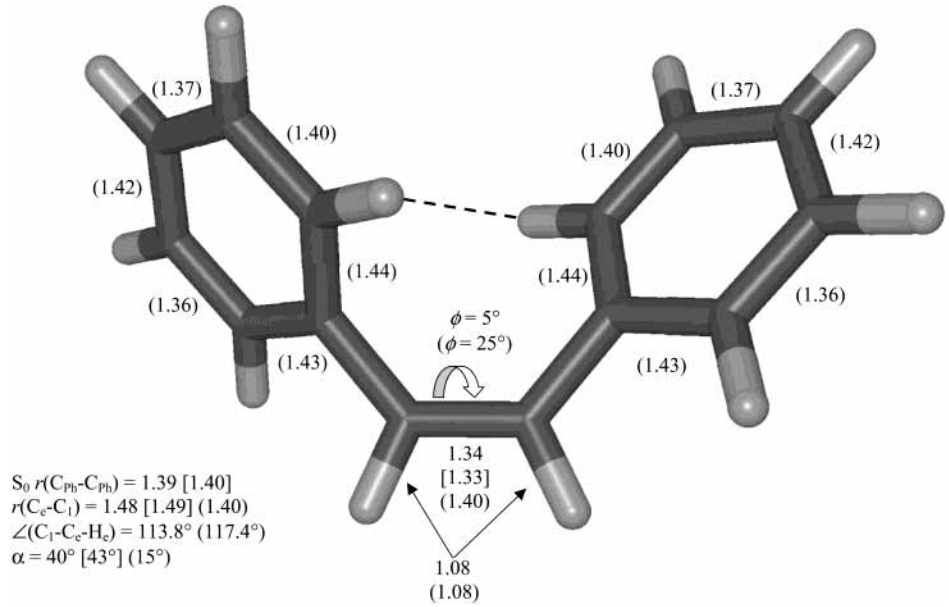

Figure 2. The S_0 equilibrium structure in the cis conformation, optimized at the SA-2-CAS(2/2) level. Geometrical parameters in parentheses are for the cis-like minimum on the lowest $\pi\rightarrow\pi^*$ excited electronic state, which is S_1 at this level of theory. Parameters in square brackets are taken from gas-phase electron diffraction experiments.[66] Ground state *cis*-stilbene is twisted slightly about the ethylenic bond to overcome steric hindrance of the phenyl ring hydrogen atoms (dashed line). After photoexcitation, the $C_1-C_e-C_{e'}-C_{1'}$ bond length alternation is lost, and the molecule twists further.

The ultrafast decay of photoexcited *cis*-stilbene motivates a search for minimal energy conical intersections of S_0 and S_1 (the ground and first excited-state potential surfaces) which lead to product formation. Bearpark and co-workers[86] reported several such intersections, obtained using molecular mechanics-valence bond (MMVB) theory. One of these was energetically accessible from the Franck−Condon region and was proposed to lead to DHP formation. Because the MMVB method does not include ionic states, only a subset of the relevant intersections can be described with this method. Amatatsu[87] reported a conical intersection obtained with limited basis sets and ab initio quantum chemistry, but gave very little information on its geometrical structure. We searched for conical intersections using the method of Bearpark et al.[88] as implemented in MOLPRO, which simultaneously minimizes the energy of the upper electronic state and the electronic energy gap. The lowest energy S_0/S_1 intersection that we located is pictured in Figure 3. The structure is twisted by 90° and has significant pyramidalization of one of the ethylenic carbon atoms. This geometry is strikingly similar to the minimal energy conical intersection of ethylene,[83] therefore we use the same label, Pyr-CI. The stilbene Pyr-CI geometry has a $C_e-C_{e'}$ bond length (1.39 Å) which is identical to that found in the ethylene Pyr-CI geometry using an SA-2-CAS(2/2) wave function and the 6-31G basis set. In Figure 4, we provide a detailed comparison of the ethylene and stilbene Pyr-CI minimal energy intersections. Hydrogen migration character is present in both the ethylene and stilbene intersections, as indicated by one extended C−H bond length. This is reminiscent of the ethylene intersection found by Ohmine,[89] and is discussed further below. To ensure

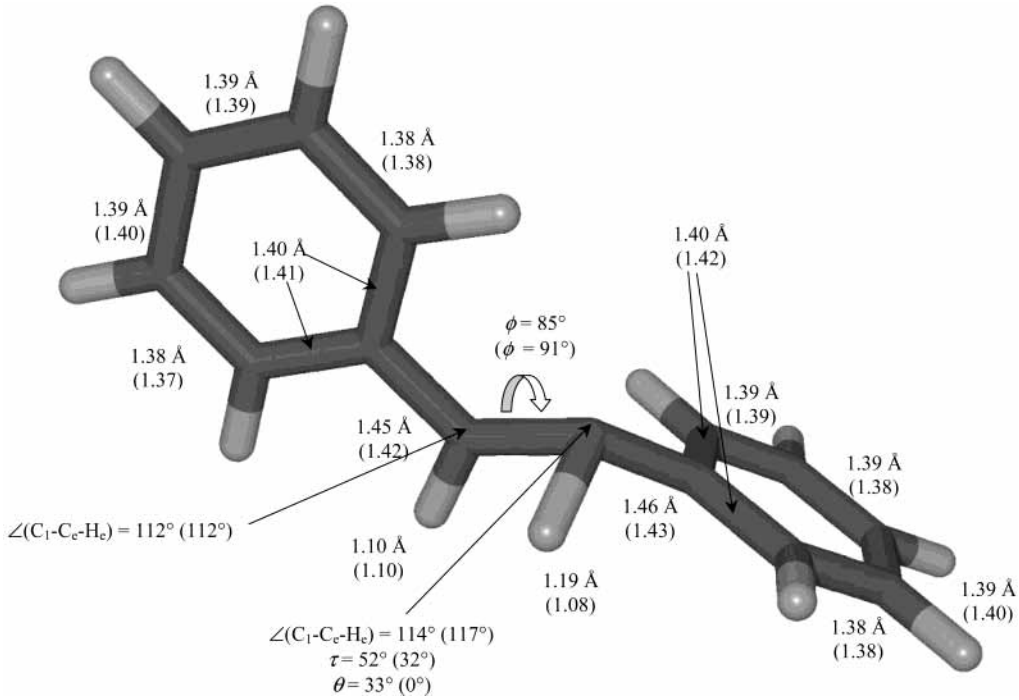

Figure 3. The lowest energy ("pyramidalized") S_0/S_1 conical intersection (Pyr-CI) found for stilbene at the SA-2-CAS(2/2) level. Geometrical parameters for both the S_0/S_1 conical intersection and the S_1 global minimum (in parentheses) are shown. Note the extended C_e-H bond length in this Pyr-CI geometry, indicating some hydrogen migration character.

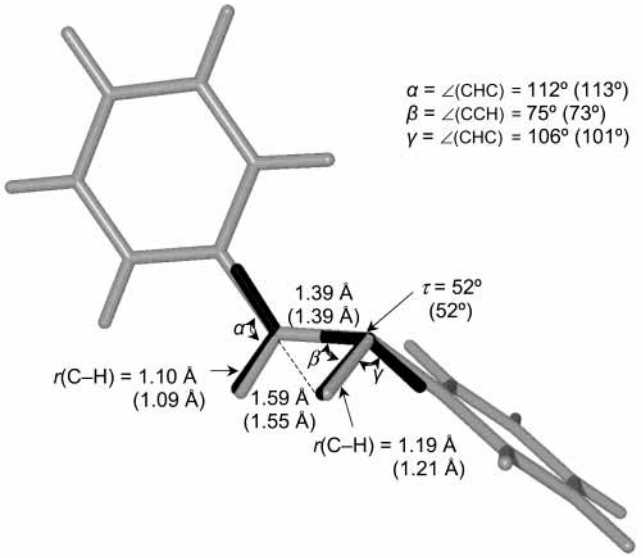

Figure 4. Comparison of geometries of SA-2-CAS(2/2) pyramidalized minimal energy conical intersections (Pyr-CI) for ethylene (black) and stilbene (gray). Geometrical parameters in parentheses correspond to the ethylene Pyr-CI geometry.

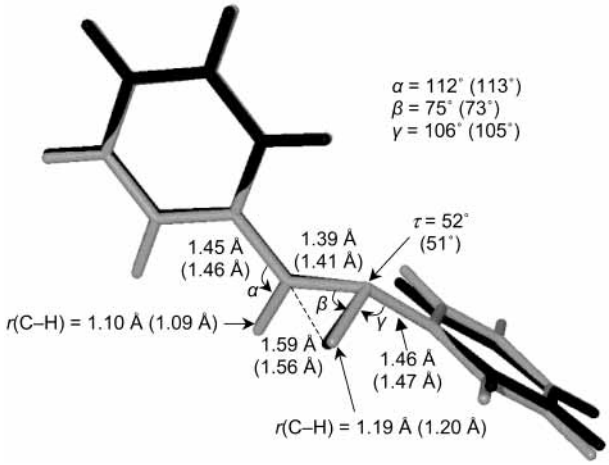

Figure 5. Geometries of SA-2-CAS(2/2) and SA-2-CAS(14/12) minimal energy conical intersections Pyr-CI in gray and black, respectively. Geometrical parameters in parentheses correspond to the SA-2-CAS(14/12) geometry.

that these similarities are not an artifact of the limited active space, we have also optimized the geometry of a minimal energy conical intersection using SA-2-CAS(14/12). The geometry is essentially unchanged, and we compare the SA-2-CAS(2/2) and SA-2-CAS(14/12) Pyr-CI geometries in Figure 5. We have also refined these Pyr-CI geometries using the larger 6-31G* and 6-31G** basis sets and the SA-2-CAS(2/2) electronic wave function. The resulting geometries differ very little from those obtained with the smaller basis sets, so will not be discussed in any detail. However, we list the 6-31G** results explicitly in the accompanying Supporting Information.

In Figure 6, we collect the energetic information for distinguished points along the reaction path. Starting from either cis or trans isomeric forms, there are nearly planar minima on the $\pi \rightarrow \pi^*$ electronic state. The geometric parameters characterizing these are given in Figures 1 and 2 for the cis-like and trans-like S_0 and S_1 minima. We cannot exclude the existence of multiple cis-like minima and we have not characterized the barrier heights for torsion on S_1.

As mentioned above, the absolute minimum on S_1 in ethylene is not a true minimum, but rather a conical intersection. We have reported a similar situation for retinal protonated Schiff base, where S_1 minima corresponding to twisting about different double bonds were either exactly or practically (within 1 kcal/mol) degenerate with a nearby conical intersection.[90,91] It is not clear whether this should be expected in general, and hence it is interesting to investigate this in some detail in the present case. The calculations described above find a clear distinction between a true minimum on S_1 and the Pyr-CI minimal energy

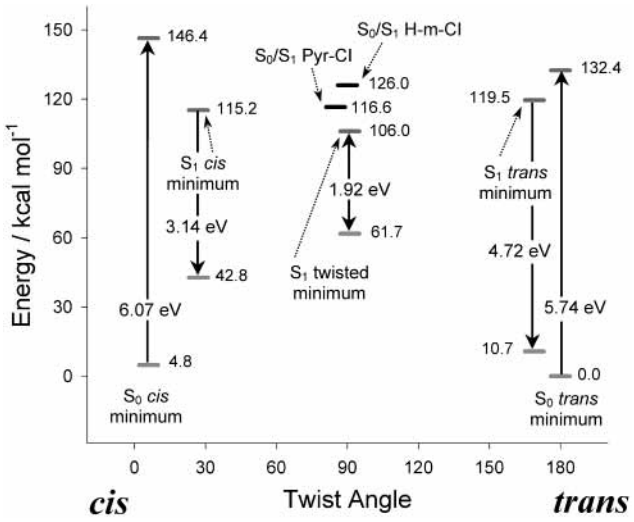

Figure 6. Important points along the reaction path in the photochemistry of stilbene, computed at the SA-2-CAS(2/2) level and plotted against the average of the Ph−C═C−Ph ($C_1-C_e-C_{e'}-C_{1'}$) and H−C═C−Ph ($H_e-C_e-C_{e'}-H_{e'}$) dihedral angles. Energy differences are given in kcal/mol, except where explicitly stated. From either the cis or trans S_0 minimum, the reaction coordinate involves primarily bond alternation, torsion, and pyramidalization as the molecule proceeds from the Franck−Condon point to the S_1 local minimum to the S_1 twisted global minimum (which is slightly pyramidalized) to the S_0/S_1 conical intersection, respectively.

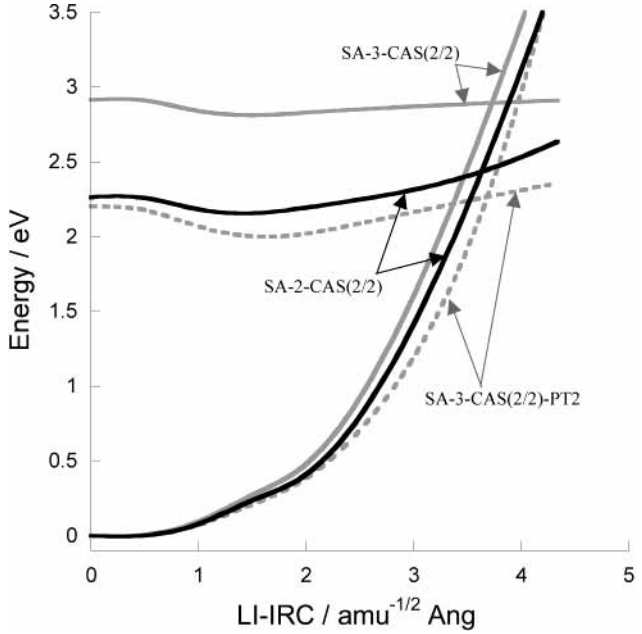

Figure 7. Reaction path from (left to right) the minimum energy purely twisted geometry to the S_1 global minimum to the twisted/pyramidalized minimal energy conical intersection. The path is linearly interpolated in internal coordinates between the stated geometries which were optimized using SA-2-CAS(2/2) wave functions in a 6-31G basis set. The path is extended slightly beyond the Pyr-CI geometry by extrapolation of the path from the global minimum to the Pyr-CI geometry. Black and gray solid lines are CAS(2/2) results state-averaging over S_0/S_1 or $S_0/S_1/S_2$, respectively. The gray dotted lines correspond to SA-3-CAS-(2/2) with second-order perturbation theory corrections. All energies are referenced to the S_0 energy at the purely twisted geometry for the given level of theory.

intersection in stilbene. Furthermore, the true minimum on S_1 is not a purely twisted geometry as has often been assumed. To investigate this further, we have carried out CASPT2 calculations including dynamic correlation.[92] The CASPT2 calculations correlated all valence electrons and used a level shift of 0.3 au. We found that the CASPT2 correction switches the CASSCF ordering of S_1 and S_2 at the Min_{90} purely twisted geometry (which is defined as the minimum on S_1 subject to the constraint that the $H_eC_eC_{e'}C_{1'}$ and $H_{e'}C_{e'}C_eC_1$ dihedral angles are 90°.) Hence SA-2-CAS(2/2)-PT2 results are not meaningful for this geometry and only SA-3-CAS(2/2) wave functions are used in the CASPT2 calculations. In Figure 7, we show the S_0 and S_1 energies along a reaction coordinate, linearly interpolated in internal coordinates from the Min_{90} purely twisted geometry to the global minimum on S_1 (Min_G) to the Pyr-CI intersection and extrapolating slightly beyond the Pyr-CI geometry. The geometries used in the interpolation all come from SA-2-CAS-(2/2) optimizations in the 6-31G basis set as discussed above. The CASSCF results are shown as black and gray solid lines for SA-2-CAS(2/2) and SA-3-CAS(2/2), respectively. The dotted gray lines are obtained with the SA-3-CAS(2/2)-PT, and are in good qualitative agreement with the SA-2-CAS(2/2) results. Dynamical correlation tends to deepen the global minimum, strengthening our conclusion that the purely twisted geometry is not a true minimum.

We have further investigated this point by carrying out SA-2-CAS(2/2) geometry optimizations using the 6-31G, 6-31G*, and 6-31G** basis sets, followed with CASPT2 corrections at the optimized geometries. The results are summarized in Table 1. The S_0/S_1 energy gap at the purely twisted geometry is only mildly sensitive to basis set and dynamic correlation. As seen for dynamic correlation effects in Figure 7, increased basis set flexibility also strengthens the conclusion that the true minimum on S_1 is pyramidalized, which can be seen in Table 1 as a decrease in ΔE_{S1} Min_G-Min_{90}. This also tends to bring the S_1 global minimum closer in energy to the conical intersection, such that the minimum and intersection are separated by less than 1 kcal/mol when using SA-3-CAS(2/2) in the largest basis set, compared to ≈10 kcal/mol with SA-2-CAS(2/2)/6-31G. Possibly larger basis sets and more extensive accounting of dynamic correlation would make the Pyr-CI an absolute minimum on S_1, but this cannot be said definitively on the basis of our present results. It is, however, safe to say that the S_1 potential energy surface in the twisted region is considerably flatter than that in ethylene, which may have consequences for the excited-state lifetime as discussed below.

Our previous studies demonstrated that the photodynamics of ethylene is dominated by both twisting (ϕ) and pyramidalization (τ),[14,16,17,83] with $S_1 \rightarrow S_0$ quenching occurring close to the minimal energy Pyr-CI geometry. Dynamics on the excited electronic state was dominated by intramolecular electron transfer connected to the degree of pyramidalization in the molecule. To further compare the photochemistry of stilbene and ethylene and investigate the importance of intramolecular electron transfer, we calculated PESs as a function of ϕ and τ for both molecules. These are shown in Figure 8, where all internal coordinates except the displayed twist and pyramidalization angles were kept fixed at the values of the optimized Pyr-CI. As expected, the plot shows that twisting (especially from the cis region) plays a large role in stabilizing photoexcited stilbene. What is commonly called the "phantom" state[20−22,93,94] corresponds to the low energy region of S_1 localized around the global minimum and close to the Pyr-CI geometry. Displacement from the global minimum along the pyramidalization coordinate toward the conical intersection requires 10.6 kcal/mol at the SA-2-CAS(2/2) level of theory and is lowered slightly to 9.2 kcal/mol using SA-2-CAS(14/12) wave functions at the SA-2-CAS(2/2) optimized geometries. This is in contrast to ethylene, where the absolute minimum on the S_1 PES *is* the

TABLE 1: Basis Set and Dynamic Correlation Effects on S_0 and S_1 Potential Energy Surfaces in the 90° Twisted Region[a]

	$\Delta E_{S_0-S_1}$ Min_{90}/eV			ΔE_{S_1} Min_G-Min_{90}/kcal mol^{-1}			ΔE_{S_1} PyrCI-Min_G/kcal mol^{-1}		
		SA-3-CAS(2/2)			SA-3-CAS(2/2)			SA-3-CAS(2/2)	
	SA-2-CAS(2/2)	CAS	CASPT2	SA-2-CAS(2/2)	CAS	CASPT2	SA-2-CAS(2/2)	CAS	CASPT2
6-31G	2.26	2.91	2.20	−2.51	−2.38	−4.59	10.55	6.13	12.60
6-31G*	2.15	2.80	2.00	−4.49	−4.58	−6.73	4.71	1.45	7.71
6-31G**	2.13	2.80	2.00	−4.39	−4.43	−7.07	4.04	0.61	7.52

[a] Min_{90} refers to the minimum energy geometry obtained while constraining the $H_e-C_e-C_e-H_e$ dihedral angles to 90°. Min_G refers to the global minimum geometry on S_1, which is twisted about the ethylenic bond and also somewhat pyramidalized around an ethylenic carbon atom. PyrCI refers to the minimum energy S_0/S_1 conical intersection, which is more strongly pyramidalized than the Min_G geometry. All geometries are optimized within the specified basis set using an SA-2-CAS(2/2) electronic wavefunction. Note that all levels of theory predict that the global minimum on S_1 is not rigidly twisted, but also pyramidalized. Furthermore, the PyrCI conical intersection geometry is higher in energy and distinct from the S_1 global minimum.

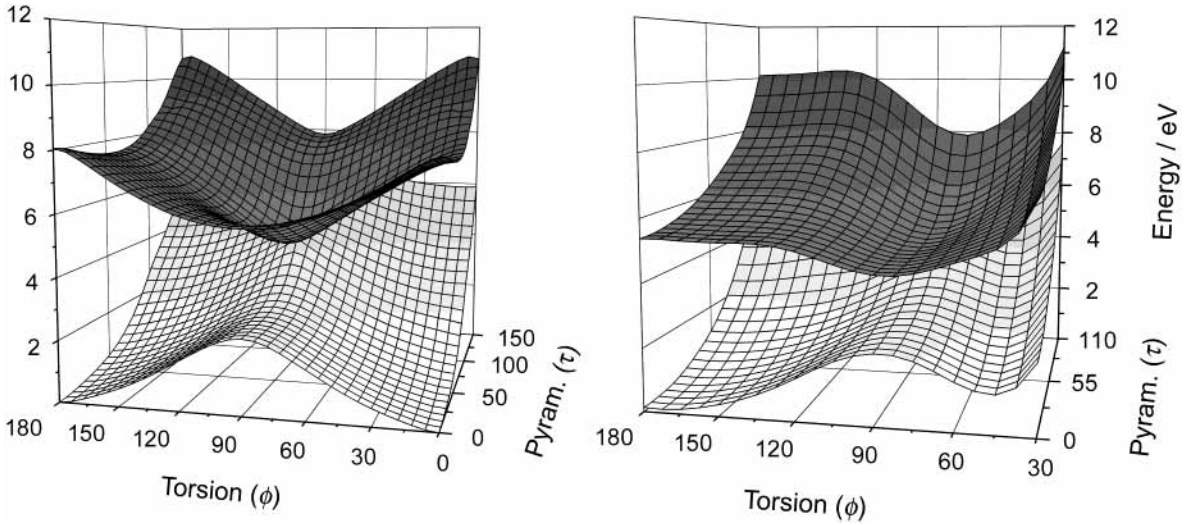

Figure 8. The ground and first excited electronic states of ethylene (left panel) and stilbene (right panel), computed using the SA-2-CAS(2/2) wave function, as a function of the twist (ϕ) and pyramidalization (τ) angles defined in Scheme 1. All other dimensions are kept at the values for the "pyramidalized" conical intersection. On the ground state of stilbene there are two minima corresponding to the cis and trans isomers. For both stilbene and ethylene, the twisted geometry represents a saddle-point on S_0. Accessing the minimal energy conical intersection from the purely twisted photoexcited molecule requires displacement along the pyramidalization coordinate.

Pyr-CI geometry. As shown in Figure 7 and Table 1, increased basis set flexibility and dynamic correlation both tend to make the global minimum on S_1 closer in energy to the Pyr-CI geometry, but these remain distinct. We conclude that the S_1 potential energy surface in the twisted pyramidalized region has a less strong funnel character compared to ethylene, suggesting that the excited-state lifetime of stilbene could be significantly longer than that of ethylene, even after accounting for the kinematic effects expected from the increased mass of the phenyl rings compared to a hydrogen atom. However, detailed dynamical studies are required to determine the magnitude of this effect, which will depend sensitively on the rate of vibrational energy redistribution.

To further characterize the Pyr-CI we calculated the S_0 and S_1 PESs as a function of displacement along the $\vec{g}$ and $\vec{h}$ vectors, as shown in Figure 9. These coordinates define the conical intersection and they describe the motions which lift the electronic state degeneracy most efficiently. They correspond to the nonadiabatic coupling ($\vec{h}$) and energy difference gradient ($\vec{g}$) as defined previously.[95,96] In the classification introduced by Ruedenberg and co-workers,[97] this intersection has a somewhat sloped topography, which could have consequences for the excited-state lifetime in dynamical simulations, as has been discussed by several authors.[91,97−99]

We have previously emphasized the role of charge transfer in the states involved in the electronic quenching of ethylene[14,16,17] and retinal protonated Schiff base.[90] Such behavior

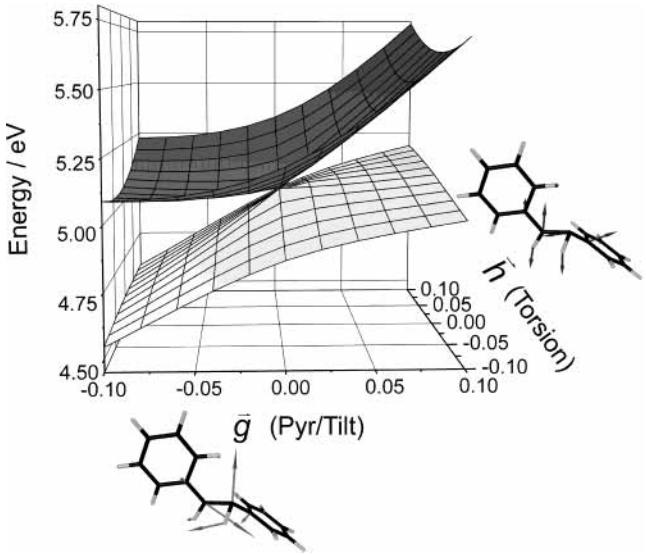

Figure 9. The ground and first excited electronic states of stilbene in the vicinity of the minimal energy conical intersection. The x and y axes represent displacement along the $\vec{g}$ and $\vec{h}$ collective coordinates, which are depicted in arrow notation.

is again seen in stilbene, as demonstrated in Figure 10, where we show the magnitude of the molecular dipole moment as a function of displacement from the conical intersection along the energy difference gradient collective coordinate. The dipole

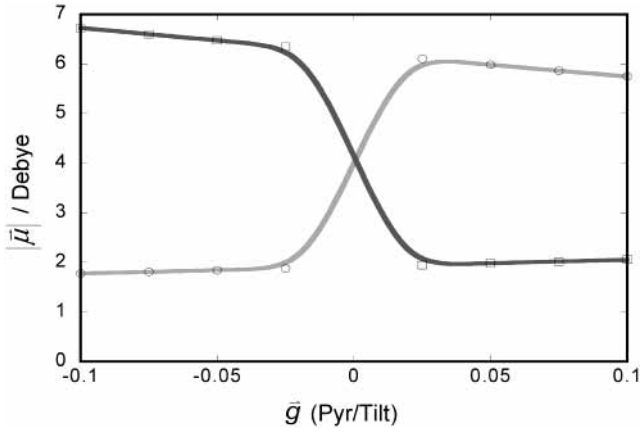

Figure 10. The dipole moment of the S_0 (light line) and S_1 (dark line) states of stilbene as a function of displacement along the $\vec{g}$ vector from the minimal energy pyramidalized conical intersection.

moment for both states is nonzero in the immediate vicinity of the intersection, but it is much larger for one state than for the other. The two states switch roles at the intersection. This suggests that the Pyr-CI intersection comes from a covalent/zwitterionic state crossing, paralleling the behavior observed in ethylene. A similar observation was made by Amatatsu,[87] suggesting that the intersection he described is essentially the Pyr-CI geometry discussed here.

As mentioned above, close inspection of the H-migration character of the Pyr-CI conical intersections reveals a tendency of one of the ends of the ethylenic bond to tilt so that the $H_e-C_e-C_{e'}$ bond angle in the pyramidalized intersection is only 75° (compared with 73°, at SA-2-CAS(2/2)/6-31G, for that of ethylene's Pyr-CI, as shown in Figure 4.) In fact, neither the $H_e-C_e-C_{e'}$ nor the $C_1-C_e-C_{e'}$ bond angles have values typical of sp^2 or sp^3 hybidization. To study this further and examine the surface topologies surrounding the conical intersections, we calculated S_0 and S_1 as a function of the tilt (τ) and pyramidalization (θ) coordinates defined in Scheme 1. The twist angle is set to 85° (the value at the Pyr-CI geometry), and the molecule end has no tilt when the $H_e-C_e-C_{e'}$ and $C_1-C_e-C_{e'}$ bond angles are equal. Displacement of the tilt angle from 0° requires rotation of the H_e atom and $C_{1-6}H_{2-6}$ phenyl group around the projection of the $H_e-C_e-C_1$ bisector onto the plane normal to the $C_{e'}-C_e$ bond. To generate the geometries for the surface we pyramidalized first and then tilted. All bond lengths, angles, and dihedral angles not involved in tilting or pyramidalization were kept fixed at the values optimized for the Pyr-CI geometry. This procedure was applied to both ethylene and stilbene using the SA-2-CAS(2/2) method. The results are compared in Figure 11.

While the energy spacing of the surfaces differs for ethylene and stilbene, the qualitative topographies are quite similar. Each contains a seam of points where the S_0 and S_1 states are close in energy. Contours of the S_0/S_1 energy difference in this coordinate space are shown below the surfaces in Figure 11. These plots expose both the pyramidalized and H-migration intersections, and clarify our understanding of S_0/S_1 coupling in these molecules. The H-migration intersection (H−*m*−CI) was first found by Ohmine, who thought it was a minimal energy intersection.[89] Even though this turned out not to be the case, nevertheless H-migration character does play a role in the Pyr-CI minimal energy intersection, and the H−*m*−CI and Pyr-CI intersections are closely related. Indeed, shortening the C−C bond length to 1.01 Å in ethylene produces a surface (not shown) where the two conical intersections nearly coalesce. In Figure 6, we have labeled the minimal energy H−*m*−CI geometry, obtained by demanding that the molecule be perfectly twisted with no pyramidalization. We emphasize that this is *not* a minimal energy conical intersection if pyramidalization is allowed. In fact, the two intersections seem to belong to the same seam of intersections, with the H-migration intersections representing a "transition state" if one moves along the seam between pyramidalized intersections. For ethylene, this has been previously suggested by several authors[83,100] and recently confirmed.[101]

Conclusions

We have investigated the S_0 and S_1 potential energy surfaces of stilbene in the region of the twisted minimum in order to determine the generality (or lack thereof) of the photoisomerization mechanism suggested by first-principles quantum dynamics simulations of ethylene photochemistry.[14,16,17] We showed that the similarities are striking and that there is much reason to believe a simple torsional reaction coordinate is not sufficient to describe stilbene photodynamics, regardless of whether one begins with the cis or trans isomer. Pyramidalization of one of the ethylenic carbon atoms was shown to be a

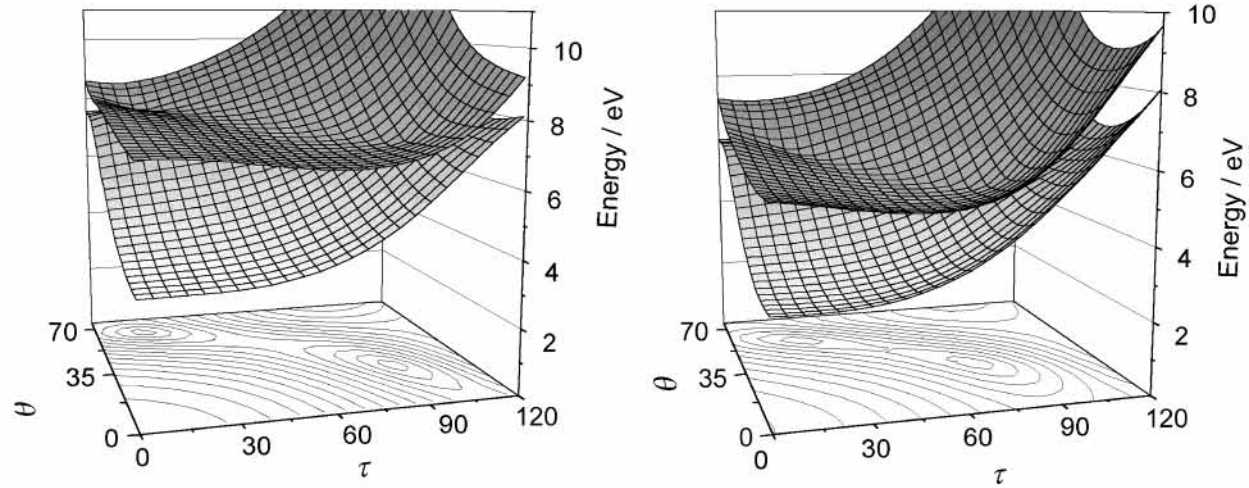

Figure 11. The ground and first excited electronic state potential energy surfaces of ethylene (left panel) and stilbene (right panel), calculated with the SA-2-CAS(2/2) wave function, as a function of the tilt (θ) and pyramidalization (τ) angles, as defined in Scheme 1. All other coordinates are fixed at the values of the "pyramidalized" conical intersection, including the perpendicular twist angle. The projected contour surface is the potential energy difference of the two states, $E(S_1) - E(S_0)$.

prerequisite for efficient nonradiative transitions from S_1 to S_0, leading to a conical intersection (Pyr-CI) and paralleling previous results for ethylene. In both ethylene and stilbene, this intersection is energetically accessible from the Franck−Condon region and is the minimal energy S_0/S_1 intersection, leading one to expect it to play a significant role in the electronic quenching.

Unlike most previous suggestions of multidimensionality in the stilbene photoisomerization reaction coordinate, our results do not stress the Franck−Condon region but rather the intersection region important to nonradiative decay. In no way does this challenge the validity of previous suggestions. Rather it is a reflection of our primary inquiry in this paper—to what extent does ethylene serve as a faithful model of photoinduced cis−trans isomerization in conjugated hydrocarbons? Clearly, the relevance of ethylene as a prototype for stilbene photisomerization will be most appropriate when steric effects engendered by the phenyl rings are minimized. The present results suggest this is obtained almost perfectly once the molecule exits the Franck−Condon region and passes over the torsional barriers.

In this respect, it is now appropriate to highlight the differences. First, there is no barrier to torsion in ethylene, while such barriers are clearly established (and reproduced but not quantified here) for stilbene. These barriers have been interpreted as arising from either the interaction of an optically dark ^1A_g state with the optically accessed ^1B_u state,[20,21] or the lowest ^1B_u state with the higher-lying 2^1B_u state.[36] We have made no comment on this aspect of the photochemistry up to this point, but the experimental consequences of these barriers clearly include a lengthening of the excited state lifetime. Second, the Pyr-CI geometry is the global minimum in ethylene, but is energetically distinct from the global minimum in stilbene. This should lead to a lengthening of the lifetime of the "phantom state," but in the absence of dynamics we cannot say by how much. The entirety of the excited-state lifetime in ethylene, making no distinction between the Franck−Condon region and the phantom state, is predicted to be less than 200 fs. Ground-state recovery experiments in solution have placed an upper bound on the stilbene "phantom state" lifetime of $\approx$150 fs.[32] Because of the zwitterionic/covalent character of the Pyr-CI intersection, polarizability of the solvent environment is likely to decrease the energy required to reach the Pyr-CI geometry from the S_1 phantom state minimum and in fact these may coincide for sufficiently polar solvents. This would decrease the excited-state lifetime relative to the gas phase. Detailed dynamical simulations now underway will allow us to quantitatively address this point. Finally, *cis*-stilbene has a photocyclization pathway, for which there is no direct analogue in ethylene.

These differences all contribute to the distinct photochemistry of stilbene compared to ethylene. However, once the excited stilbene molecule proceeds far enough along the torsional coordinate to pass over the torsional barriers and bypass the photocyclization pathway, the picture given in this paper shows that the key considerations in the electronic quenching of stilbene and ethylene are very similar. The Pyr-CI intersection in both ethylene and stilbene arises from the interaction of covalent and charge-transfer states, implying that the lifetime of the phantom state can be modified by a charged environment. We have pointed out the role of the tilting coordinate which connects the Pyr-CI intersection to H-migration intersections in both ethylene and stilbene. The combination of pyramidalization, twisting, and tilting, which is required to reach the Pyr-CI intersection, suggests a reaction coordinate which will have the qualitative "slicing" character that Fleming and co-workers have predicted on the basis of measurements of viscosity effects on photoisomerization rates from the cis isomer.[28]

The most important point in this paper is that the two-coordinate (torsion and pyramidalization) and three-state (N, V, and Z) model we have proposed for ethylene is also appropriate for stilbene once the twisted region ("phantom state") is reached. Considering also the CASPT2 results for styrene,[18] one can conclude that this model is appropriate for three of the most paradigmatic cis−trans photoisomerization molecules. It will be interesting to carry out ab initio molecular dynamics of photoexcited stilbene and to further characterize the photocyclization pathway. These studies are currently underway.

Acknowledgment. This work was supported by the U.S. Department of Energy through the University of California under Subcontract B341494 and the National Science Foundation (NSF CHE-97-33403.) T.J.M. is a Beckman Young Investigator, Packard Fellow, Sloan Fellow, and a Dreyfus Teacher-Scholar. We thank the National Computer Science Alliance for computational resources on the SGI/Cray Origin 2000 provided through Grant CHE020014N. We are also grateful to Prof. M. Merchan for a critical reading of the manuscript and helpful suggestions.

Supporting Information Available: Cartesian coordinates and energies of structures described in the text and the collective coordinates used in Figure 9 are available. This material is available free of charge via the Internet at http://pubs.acs.org.

References and Notes

(1) Pullen, S.; Walker, L. A., II; Donovan, B.; Sension, R. J. *Chem. Phys. Lett.* **1995**, *242*, 415.
(2) Pullen, S. H.; Anderson, N. A.; Walker, L. A., II; Sension, R. J. *J. Chem. Phys.* **1997**, *107*, 4985.
(3) Pullen, S. H.; Anderson, N. A.; Walker, L. A., II; Sension, R. J. *J. Chem. Phys.* **1998**, *108*, 556.
(4) Anderson, N. A.; Pullen, S. H.; Walker, L. A., II; Shiang, J. J.; Sension, R. J. *J. Phys. Chem. A* **1998**, *102*, 10588.
(5) Anderson, N. A.; Durfee, C. G., III; Murnane, M. M.; Kapteyn, H. C.; Sension, R. J. *Chem. Phys. Lett.* **2000**, *232*, 365.
(6) Lochbrunner, S.; Fuss, W.; Kompa, K. L.; Schmid, W. E. *Chem. Phys. Lett.* **1997**, *274*, 491.
(7) Lochbrunner, S.; Fuss, W.; Schmid, W. E.; Kompa, K. L. *J. Phys. Chem. A* **1998**, *102*, 9334.
(8) Fuss, W.; Schikarski, T.; Schmid, W. E.; Trushin, S. A.; Hering, P.; Kompa, L. *J. Chem. Phys.* **1997**, *106*, 2205.
(9) Greene, B. I.; Farrow, R. C. *J. Chem. Phys.* **1983**, *76*, 3336.
(10) Baumert, T.; Frohnmeyer, T.; Kiefer, B.; Niklaus, P.; Strehle, M.; Gerber, G.; Zewail, A. H. *Appl. Phys. B* **2001**, *72*, 105.
(11) Pederson, S.; Banares, L.; Zewail, A. H. *J. Chem. Phys.* **1992**, *97*, 8801.
(12) Farmanara, P.; Stert, V.; Radloff, W. *Chem. Phys. Lett.* **1998**, *288*, 518.
(13) Mestdagh, J. M.; Visticot, J. P.; Elhanine, M.; Soep, B. *J. Chem. Phys.* **2000**, *113*, 237.
(14) Ben-Nun, M.; Quenneville, J.; Martínez, T. J. *J. Phys. Chem. A* **2000**, *104*, 5161.
(15) Michl, J.; Bonacic-Koutecky, V. *Electronic Aspects of Organic Photochemistry*; Wiley-Interscience: New York, 1990.
(16) Ben-Nun, M.; Martínez, T. J. *Chem. Phys. Lett.* **1998**, *298*, 57.
(17) Quenneville, J.; Ben-Nun, M.; Martínez, T. J. *J. Photochem. Photobiol. A* **2001**, *144*, 229.
(18) Molina, V.; Merchan, M.; Roos, B. O.; Malmqvist, P.-A. *Phys. Chem. Chem. Phys.* **2000**, *2*, 2211.
(19) Saltiel, J. *J. Am. Chem. Soc.* **1967**, *89*, 1036.
(20) Orlandi, G.; Siebrand, W. *Chem. Phys. Lett.* **1975**, *30*, 352.
(21) Tavan, P.; Schulten, K. *Chem. Phys. Lett.* **1978**, *56*, 200.
(22) Waldeck, D. H. *Chem. Rev.* **1991**, *91*, 415.
(23) Park, N. S.; Waldeck, D. H. *Chem. Phys. Lett.* **1990**, *168*, 379.
(24) Lee, M.; Haseltine, J. N.; Smith, A. B., III; Hochstrasser, R. M. *J. Am. Chem. Soc.* **1989**, *111*, 5044.
(25) Todd, D. C.; Jean, J. M.; Rosenthal, S. J.; Ruggiero, A. J.; Yang, D.; Fleming, G. R. *J. Chem. Phys.* **1990**, *93*, 8658.

(26) Abrash, S.; Repinec, S.; Hochstrasser, R. M. *J. Chem. Phys.* **1990**, *93*, 1041.
(27) Rodier, J.-M.; Myers, A. B. *J. Am. Chem. Soc.* **1993**, *115*, 10791.
(28) Todd, D. C.; Fleming, G. R.; Jean, J. M. *J. Chem. Phys.* **1992**, *97*, 8915.
(29) Myers, A. B.; Mathies, R. A. *J. Chem. Phys.* **1984**, *81*, 1552.
(30) Repinec, S. T.; Sension, R. J.; Szarka, A. Z.; Hochstrasser, R. M. *J. Phys. Chem.* **1991**, *95*, 10380.
(31) Sension, R. J.; Szarka, A. Z.; Hochstrasser, R. M. *J. Chem. Phys.* **1992**, *97*, 5239.
(32) Sension, R. J.; Repinec, S. T.; Szarka, A. Z.; Hochstrasser, R. M. *J. Chem. Phys.* **1993**, *98*, 6291.
(33) Szarka, A. Z.; Pugliano, N.; Palit, D. K.; Hochstrasser, R. M. *Chem. Phys. Lett.* **1995**, *240*, 25.
(34) Muszkat, K. A.; Fisher, E. *J. Chem. Soc. B* **1967**, 662.
(35) Petek, H.; Yoshihara, K.; Fujiwara, Y.; Lin, Z.; Penn, J. H.; Frederick, J. H. *J. Phys. Chem.* **1990**, *94*, 7539.
(36) Molina, V.; Merchan, M.; Roos, B. O. *Spectrosc. Acta A* **1999**, *55*, 433.
(37) Warshel, A. *J. Chem. Phys.* **1975**, *62*, 214.
(38) Frederick, J. H.; Fujiwara, Y.; Penn, J. H.; Yoshihara, K.; Petek, H. *J. Phys. Chem.* **1991**, *95*, 2845.
(39) Berweger, C. D.; van Gunsteren, W. F.; Muller-Plathe, F. *J. Chem. Phys.* **1998**, *108*, 8773.
(40) Berweger, C. D.; van Gunsteren, W. F.; Muller-Plathe, F. *J. Chem. Phys.* **1999**, *111*, 8987.
(41) Berweger, C. D.; van Gunsteren, W. F.; Muller-Plathe, F. *Angew. Chem., Int. Ed.* **1999**, *38*, 2609.
(42) Vachev, V. D.; Frederick, J. H.; Grishanin, B. A.; Zadkov, V. N.; Koroteev, N. I. *Chem. Phys. Lett.* **1993**, *215*, 306.
(43) Vachev, V. D.; Frederick, J. H.; Grishanin, B. A.; Zadkov, V. N.; Koroteev, N. I. *J. Phys. Chem.* **1995**, *99*, 5247.
(44) Negri, F.; Orlandi, G. *J. Phys. Chem.* **1991**, *95*, 748.
(45) Banares, L.; Heikal, A. A.; Zewail, A. H. *J. Phys. Chem.* **1992**, *96*, 4127.
(46) Nordholm, S. *Chem. Phys.* **1989**, *137*, 109.
(47) Bolton, K.; Nordholm, S. *Chem. Phys.* **1996**, *203*, 101.
(48) Heikal, A. A.; Baskin, J. S.; Banares, L.; Zewail, A. H. *J. Phys. Chem. A* **1997**, *101*, 572.
(49) Gershinsky, G.; Pollak, E. *J. Chem. Phys.* **1996**, *105*, 4388.
(50) Gershinsky, G.; Pollak, E. *J. Chem. Phys.* **1997**, *107*, 10532.
(51) Leitner, D. M.; Wolynes, P. G. *Chem. Phys. Lett.* **1997**, *280*, 411.
(52) Kim, S. K.; Courtney, S. H.; Fleming, G. R. *Chem. Phys. Lett.* **1989**, *159*, 543.
(53) Heikal, A. A.; Chong, S. H.; Baskin, J. S.; Zewail, A. H. *Chem. Phys. Lett.* **1995**, *242*, 380.
(54) Mohrschladt, R.; Schroeder, J.; Schwarzer, D.; Troe, J.; Vohringer, P. *J. Chem. Phys.* **1994**, *101*, 7566.
(55) Schroeder, J.; Schwarzer, D.; Troe, J.; Vohringer, P. *Chem. Phys. Lett.* **1994**, *218*, 43.
(56) Schroeder, J.; Schwarzer, D.; Troe, J.; Voss, F. *J. Chem. Phys.* **1990**, *93*, 2393.
(57) Sun, Y.-P.; Saltiel, J. *J. Phys. Chem.* **1989**, *93*, 8310.
(58) Sun, Y.-P.; Saltiel, J.; Park, N. S.; Hoburg, E. A.; Waldeck, D. H. *J. Phys. Chem.* **1991**, *95*, 10336.
(59) Suzuki, T.; Mikami, N.; Ito, M. *J. Phys. Chem.* **1986**, *90*, 6431.
(60) Werner, H.-J.; Knowles, P. J.; Amos, R. D.; Bernhardsson, A.; Berning, A.; Celani, P.; Cooper, D. L.; Deegan, M. J. O.; Dobbyn, A. J.; Eckert, F.; Hampel, C.; Hetzer, G.; Korona, T.; Lindh, R.; Lloyd, A. W.; McNicholas, S. J.; Manby, F. R.; Meyer, W.; Mura, M. E.; Nicklass, A.; Palmieri, P.; Pitzer, R.; Rauhut, G.; Schütz, M.; Stoll, H.; Stone, A. J.; Tarroni, R.; Thorsteinsson, T. MOLPRO 2000.1, 2000.
(61) Hehre, W. J.; Ditchfield, R.; Pople, J. A. *J. Chem. Phys.* **1972**, *56*, 2257.
(62) Frisch, M. J.; Pople, J. A.; Binkley, J. S. *J. Chem. Phys.* **1984**, *80*, 3265.
(63) Radhakrishnan, T. P.; Agranat, I. *Struct. Chem.* **1990**, *2*, 19.
(64) Docken, K. K.; Hinze, J. *J. Chem. Phys.* **1972**, *57*, 4928.
(65) Roos, B. O. The Complete Active Space Self-Consistent Field Method and Its Applications in Electronic Structure Calculations. In *Advances in Chemical Physics: Ab Initio Methods in Quantum Chemistry II*; Lawley, K. P., Ed.; John Wiley and Sons Ltd.New York, 1987; p 399.
(66) Trætteberg, M.; Frantsen, E. B. *J. Mol. Struct.* **1975**, *26*, 69.
(67) Rice, J. K.; Baronavski, A. P. *J. Phys. Chem.* **1992**, *96*, 3359.
(68) Molina, V.; Merchan, M.; Roos, B. O. *J. Phys. Chem. A* **1997**, *101*, 3478.
(69) Spangler, L. H.; van Zee, R. D.; Blankespoor, S. C.; Zwier, T. S. *J. Phys. Chem.* **1987**, *91*, 6077.
(70) Champagne, B. B.; Pfanstiel, J. F.; Plusquellic, D. F.; Pratt, D. W.; van Herpen, W. M.; Meerts, W. L. *J. Phys. Chem.* **1990**, *94*, 6.
(71) Dyck, R. H.; McClure, D. S. *J. Chem. Phys.* **1962**, *36*, 2326.
(72) Trætteberg, M.; Frantsen, E. B.; Mijlhoff, F. C.; Hoekstra, A. *J. Mol. Struct.* **1975**, *26*, 57.
(73) Choi, C. H.; Kertesz, M. *J. Phys. Chem. A* **1997**, *101*, 3823.
(74) Arenas, J. F.; Tocon, I. L.; Otero, J. C.; Marcos, J. I. *J. Phys. Chem.* **1995**, *99*, 11392.
(75) Spangler, L. H.; van Zee, R. D.; Zwier, T. S. *J. Phys. Chem.* **1987**, *91*, 2782.
(76) Tachon, M.; Davies, E.; Lamotte, M.; Muszkat, K. A.; Wismontski-Knittel, T. *J. Phys. Chem.* **1994**, *98*, 11870.
(77) Baranovic, G.; Meic, Z.; Maulitz, A. H. *Spectrosc. Acta A* **1998**, *54*, 1017.
(78) Allen, M. T.; Whitten, D. G. *Chem. Rev.* **1989**, *89*, 1691.
(79) Ci, X.; Myers, A. B. *Chem. Phys. Lett.* **1989**, *158*, 263.
(80) Lhost, O.; Bredas, J. L. *J. Chem. Phys.* **1992**, *96*, 5279.
(81) Chiang, W.-Y.; Laane, J. *J. Chem. Phys.* **1994**, *100*, 8755.
(82) Holneicher, G.; Muller, M.; Demmer, M.; Lex, J.; Penn, J. H.; Gan, L.; Loesel, P. D. *J. Am. Chem. Soc.* **1988**, *110*, 4483.
(83) Ben-Nun, M.; Martínez, T. J. *Chem. Phys.* **2000**, *259*, 237.
(84) Garavelli, M.; Celani, P.; Bernardi, F.; Robb, M. A.; Olivucci, M. *J. Am. Chem. Soc.* **1997**, *119*, 6891.
(85) Saltiel, J.; Ganapathy, S.; Werking, C. *J. Phys. Chem.* **1987**, *91*, 2755.
(86) Bearpark, M. J.; Bernardi, F.; Clifford, S.; Olivucci, M.; Robb, M. A.; Vrevren, T. *J. Phys. Chem. A* **1997**, *101*, 3841.
(87) Amatatsu, Y. *Chem. Phys. Lett.* **1999**, *314*, 364.
(88) Bearpark, M. J.; Robb, M. A.; Schlegel, H. B. *Chem. Phys. Lett.* **1994**, *223*, 269.
(89) Ohmine, I. *J. Chem. Phys.* **1985**, *83*, 2348.
(90) Molnar, F.; Ben-Nun, M.; Martínez, T. J.; Schulten, K. *J. Mol. Struct. (THEOCHEM)* **2000**, *506*, 169.
(91) Ben-Nun, M.; Molnar, F.; Schulten, K.; Martínez, T. J. *Proc. Natl. Acad. Sci.* **2002**, *99*, 1769.
(92) Celani, P.; Werner, H.-J. *J. Chem. Phys.* **2000**, *112*, 5546.
(93) Saltiel, J.; D'Agostino, J. T. *J. Am. Chem. Soc.* **1972**, *94*, 6445.
(94) Saltiel, J.; D'Agostino, J. T.; Megarity, E. D.; Metts, L.; Neuberger, K. R.; Wrighton, M.; ZaFiriou, O. C. *Org. Photochem.* **1973**, *3*, 1.
(95) Yarkony, D. R. *Rev. Mod. Phys.* **1996**, *68*, 985.
(96) Yarkony, D. R. *Acc. Chem. Res.* **1998**, *31*, 511.
(97) Atchity, G. J.; Xantheas, S. S.; Ruedenberg, K. *J. Chem. Phys.* **1991**, *95*, 1862.
(98) Yarkony, D. R. *J. Chem. Phys.* **2001**, *114*, 2601.
(99) de Vico, L.; Page, C. S.; Garavelli, M.; Bernardi, F.; Basosi, R.; Olivucci, M. *J. Am. Chem. Soc.* **2002**, *124*, 4124.
(100) Freund, L.; Klessinger, M. *Int. J. Quantum Chem.* **1998**, *70*, 1023.
(101) Wilsey, S.; Houk, K. N. *J. Am. Chem. Soc.* **2002**, *124*, 11182.